Molecular-dynamics model of interface amorphization

Mariana Weissmann
Departamento de Física, Comisión Nacional de Energía Atómica, avenida Libertador 8250, 1429 Buenos Aires, Argentina

Ricardo Ramírez and Miguel Kiwi
Facultad de Física, Universidad Católica de Chile, Casilla 306, Santiago 22, Chile
(Received 23 December 1991)

The atomic arrangements of a metallic superlattice, such as the one formed by Co and Zr, and their redistribution with growing temperature, are studied. The Co-Zr system was reported by Schröder *et al.* to become amorphous because of a solid-state reaction. A molecular-dynamics simulation is performed, using Lennard-Jones–type interatomic potentials. The way in which disorder develops as the temperature increases is graphically displayed. The temperature at which the layers first become disordered, and subsequently melt, is found to be strongly dependent on the thickness of the slab.

I. INTRODUCTION

Metallic-glass formation through interdiffusion at an interface between two crystalline metals has attracted the interest of physicists, metallurgists, and chemists for some time.[1] Glass formation through solid-state interdifusion, in a multilayer structure of two crystalline metals, was reported[2–4] by Johnson and Schwartz in 1983, and has since been studied by several groups.[5] In particular, Schröder, Samwer, and Koster[6] studied, by electron microscopy, the metallic-glass formation at Zr-Co interfaces.

They grew a Zr (34 nm) – Co (20 nm) multilayer structure ($Zr_{45}Co_{55}$). After annealing for 2 h, at temperatures as low as 510 K, a significant interface reaction had already taken place. Maintaining the same temperature for hours, or even minutes, leads to the formation of an almost complete Co-rich amorphous microstructure, of average concentration $Zr_{20}Co_{80}$, with only a few Zr crystals remaining.

Obviously time scales of the order of hours, or even minutes, are completely outside of the realm of feasibility of molecular dynamics (MD). However, successful MD simulations of structural relaxation of an amorphous alloy have been carried out[7] within reasonable computing time. They seem to provide a consistent picture of the atomic environments, as revealed by good agreement with experiments.[8,9] In fact, it can be confirmed that after 100 MD time steps an arbitrary given velocity distribution converges to that given by the Maxwell-Boltzmann law, even at temperatures of only 100 K. A typical order of magnitude value for a MD time step is 10^{-15} s. A Debye frequency of 300 K corresponds to $\sim 1.4 \times 10^{-13}$ s and thus, to more than a hundred MD time steps, which seems quite reasonable. Consequently, one expects to be able to draw some physically valid conclusions on the basis of simulations of around 10 000 time steps, which is equivalent to $\approx 10^{-11}$ s of real time, including the study of amorphization and structural relaxation. Kobayashi and Takeuchi[7] make an even riskier assumption: they conjecture that simulated annealing in MD may be representative of experimental annealing. This implies the existence of some kind of scaling between the system size and the time it requires to reach thermodynamic equilibrium; a conjecture which has not been proved up to now.

A major issue in carrying out MD simulations is an adequate choice of the interaction potential. In fact, it has been shown that several properties may depend on the potential selected to carry out the simulation.[10] Recently, Plimpton and Wolf[11] have discussed this problem in great detail and proposed a method which gives a linear relation between barrier height and melting temperature, which turns out to be appropriate to predict diffusion coefficients and transport properties for any pair potential in fcc metals.

We choose as our potential a Lennard-Jones (LJ) pairwise interaction, modified in accordance with the spirit of Ref. 11 and incorporating information pointed out by Massobrio, Pontikis, and Martin,[12] in their study of amorphization in $NiZr_2$. Details on the precise selection of the potential are given in Sec. II.

However, the Lennard-Jones interaction potential we adopt is too simple to describe transition-metal alloys and compounds. Thus, when we speak of slabs of Co and/or Zr we only do it in a generic sense, intending to illustrate the general behavior of systems with two different atomic elements, which are spatially adjacent, and which have the atomic size and melting temperatures of Co and Zr, respectively. Consequently, our results do not pretend to model the Co-Zr system rigorously, but rather apply to a class of systems dominated by size effects, of which Co-Zr may be an example.

This paper is organized as follows: after this introduction the model is described in Sec. II. Results of the simulations, carried out for a variety of different situations, are reported in Sec. III. A summary is given and conclusions are drawn in Sec. IV, which closes this contribution.

II. MODEL

The system consists of slabs of fcc (100) layers of cobalt and zirconium parallel to the x-y plane, which provide a physical model quite close to the actual hexagonal structure. The single-crystal nearest-neighbor distances between pairs of Co and Zr atoms are 2.51 and 3.23 Å, respectively, and are taken as data to fit the potential parameters. We consider these to be of Lennard-Jones type, but with exponents 4 and 8, as suggested in his book by Harrison,[13] for transition metals. We therefore assume, for the interaction of two atoms of the same element, the potential given by

$$V(r) = \frac{A_\alpha}{r^4} + \frac{B_\alpha}{r^8} + C_\alpha r + D_\alpha, \tag{2.1}$$

where $\alpha =$ Zr or Co, and the parameters C and D were included in order to allow for a smooth potential cutoff.[11] In fact, they were chosen so that the potential goes to zero with zero gradient at $r = 2d$, where d is the position of the minimum of $V(r)$. In addition, the curvature of the potential at the minimum is determined by fitting the experimental value of the respective bulk modulus. The parameters A, B, C, and D are uniquely determined by these requirements. For the interaction between unlike atoms we have taken the geometric average of the parameters of the pure materials.

However, the magnitude of the cohesive energies of cobalt and zirconium turn out to be about one-half of the experimental values, if one retains only the sum of these pairwise interactions in the energy calculation.[12] Due to the sharp cutoff of the potential, at twice the radius which corresponds to its minimum, only up to third-neighbor interactions are nonzero for the fcc structure (first-, second-, and third-neighbor distances are d, $\sqrt{2}d$, and $\sqrt{3}d$, respectively). Moreover, second- and third-neighbor interactions are of course significantly reduced as a consequence of the cutoff. Thus, to obtain reasonable values for the cohesive energy $E_{\rm coh}$ we write it as the following sum of pairwise interactions:

$$E_{\rm coh} = 6V(d) + 3V(\sqrt{2}d) + 12V(\sqrt{3}d) + G\,, \tag{2.2}$$

where the G term is closely related to the slowly varying density-dependent attractive term of the embedded atom method.[14]

At the start of our calculations we fitted the experimental value of $E_{\rm coh}$ with $G = 0$, and ignored the experimental bulk moduli as data. But, this procedure gave unreasonable values not only for the bulk moduli, but also for the melting temperatures. However, we then realized that it was unnecessary to repeat the simulations in order to also fit the experimental values of the bulk moduli. In fact, it is enough to multiply all energies and temperatures by a constant $k < 1$, which implies a rescaling of the time intervals by a factor $1/\sqrt{k}$. Since the values of k obtained by fitting the bulk moduli of pure Co and Zr turned out to be different, we adopted an average value of $k = 0.4$ for the mixed system. Table I shows the parameters that were actually used, taking into account this multiplicative factor. They are given in nondimensional units, to be defined in Sec. III.

TABLE I. Constants for the Lennard-Jones potential.

	Co	Zr
A	−13.755	−52.087
B	51.646	523.16
C	−0.14325	−0.15398
D	0.5847	0.80864

Two features related to our potentials are interesting to notice. The first one is that they fall on the universal curve of Rose *et al.*[15] And, on the other hand, when we evaluate the fcc Zr cohesion energy as a function of the lattice parameter, it turns out to coincide with the results of Massobrio, Pontikis, and Martin[12] in spite of the fact that they go beyond pairwise potentials.

The number of atoms in the layers were chosen so as to make the misfit at the Zr-Co interface as close as possible to the experimental ratio of the lattice constants, compatible with a manageable system size. The number of atoms in one cobalt layer was chosen as $9\times9\times2 = 162$ and in zirconium as $7\times7\times2 = 98$, since $\frac{9}{7} = 1.285\ldots$ is quite close to the ratio of nearest-neighbor distances of Zr and Co atoms. Periodic boundary conditions in the x-y planes were adopted. In the z direction both a periodic and a slab geometry were investigated, for various different numbers of superimposed layers. The cell size in the z direction was obtained from simulations with the slab geometry.

At this point we once again remark that, while many of the parameters correspond to Co and Zr they are taken only as representative entities, in order to obtain physical trends. Because of the crude Lennard-Jones interaction potential we adopted, our model does not incorporate in detail all the complexity of the actual metallic Co-Zr system.

Our procedure is not as general as that of Lutsko *et al.*,[16] in that we do not incorporate the temperature dependence of the lattice parameter, that is, we limit ourselves to study a constant volume system. As will be shown below, the overall size of our system does not show a significant thermal expansion, within the temperature range we investigate, so that this shortcoming does not seem to affect our main inferences.

III. RESULTS

The molecular-dynamics (MD) simulations were implemented, for up to 50 000 time steps in every run, according to the scheme outlined in Sec. II. The time step we adopted is of 4.4×10^{-15} s, our unit of length is 1.5486 Å, and the temperatures are reported in units of ≈ 5400 K. Our interest is to trail closely the disordering process, which we do by slowly increasing the temperature. Thus, we start with a normal velocity distribution at a low-temperature value, and increment the total energy by boosting these velocities in small steps.

The most direct and convenient way to describe dis-

order is simply to display graphically the particle distributions. For example, the number of particles between z and $z+dz$, the plot of all particles close to the interface in the x-y plane, etc. However, some quantification of the degree of disorder was also implemented through the evaluation of the structure factor, the pair-correlation function, and mean square atomic deviation.

The static structure factor, i.e., the Fourier transform of the density in each crystallographic plane parallel to the interface, was calculated as suggested by Phillpot, Yip, and Wolf in Ref. 17, as a convenient way of characterizing the degree of order in a plane. It is defined as

$$S(\mathbf{K},n)=\left\langle \frac{1}{N_z^2}\left|\sum_{j=1}^{N_z}\exp(i\mathbf{K}\cdot\mathbf{r_j})\right|^2\right\rangle , \tag{3.1}$$

where n labels the crystal plane to which the points $\mathbf{r_j}$ belonged at low temperatures, and $\mathbf{K}$ is a vector of the planar reciprocal lattice [in particular, we used $\mathbf{K}=(1,1)$]. The structure factor $S=1$ for a perfectly ordered crystal and decreases to zero when complete disorder sets in. We speak of the amorphization of layer n when its structure factor $S\longrightarrow 0$. While this approach follows the spirit of the work of Phillpot, Yip, and Wolf,[17] the reservations raised by Robbins, Grest, and Kremer,[18] in their study of finite-size effects in MD simulations of melting, should be kept in mind.

Another probe of disorder is to calculate $g_2(r)$, the pair-correlation function, defined as the number of atoms between $(r,r+dr)$, provided that there is one atom at the origin. Analytically

$$g_2(r)=n(r)/n_0 , \tag{3.2}$$

where n denotes atomic density, $r=|\mathbf{r}|$, and $r=0$ defines the position of a reference atom. Still another way to characterize disorder is to evaluate the mean square deviation from the initial configuration $\langle(r-r_0)^2\rangle$, which is related to the diffusion coefficient.

The most important observation, related to the results of our simulations, is that before any interdiffusion is observed, first the interface, and then all the Co layers become completely disordered. (In this context, we denominate interdiffusion the crossing of the interface of atoms

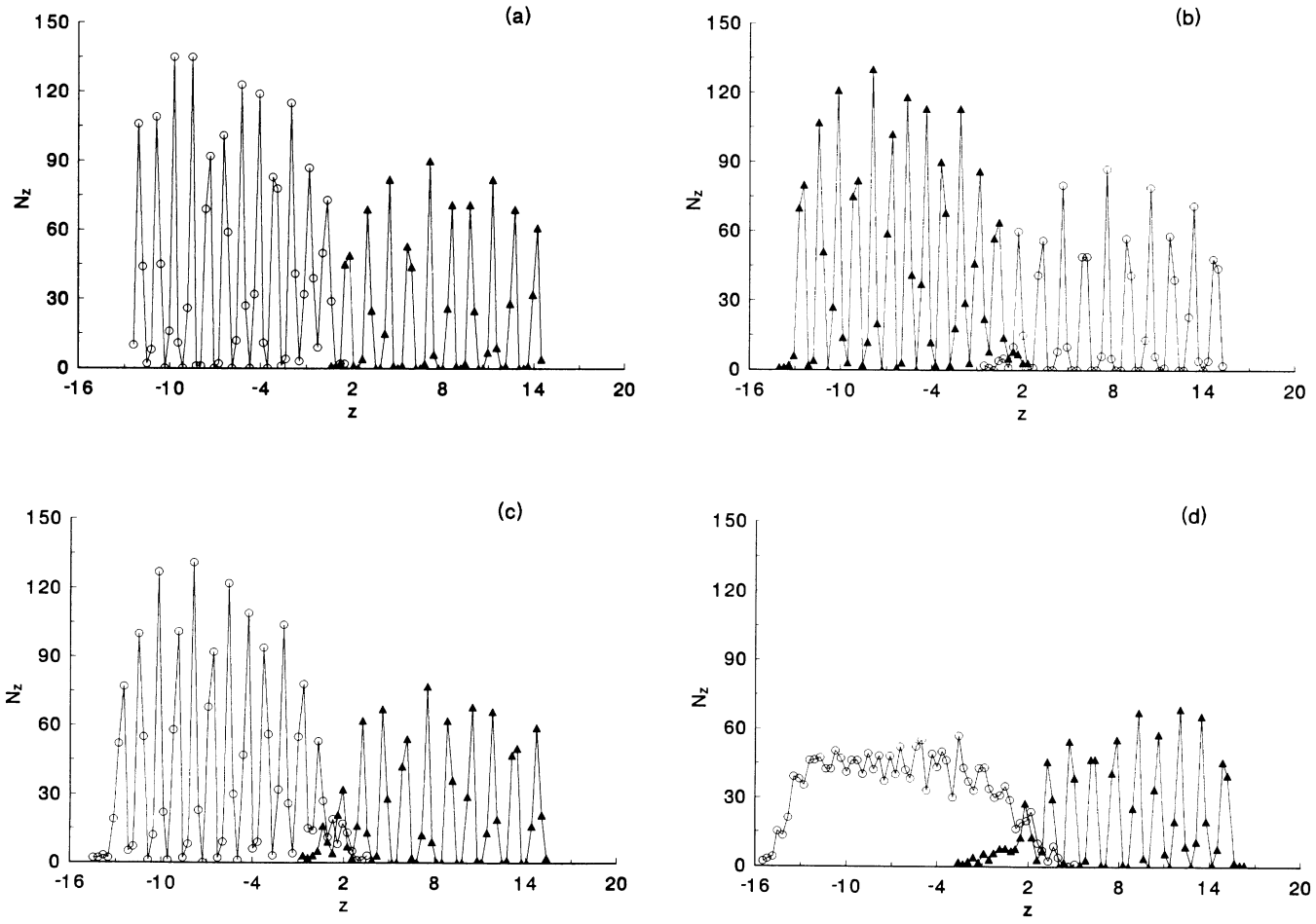

FIG. 1. Histograms of the spatial distribution of 1944 Co and 980 Zr atoms, denoted by open circles and full triangles, respectively, for various values of the temperature t after 5000 time steps. (a) $t=0.2$, (b) $t=0.24$, (c) $t=0.27$, and (d) $t=0.30$.

of one species, towards the side where originally only atoms of the other species could be found.) Of course this disordering is due to the lower melting point of Co relative to Zr, but the phenomenon is strongly enhanced because of the small number of crystal planes in each layer. This disordering temperature is very sharp, for a given number of Co planes, both in the slab geometry and when periodic boundary conditions are imposed in the z direction.

A. Slab geometry

As already mentioned, an overall feature of our computations is that the slab does not change significantly its volume. Thus, we choose to carry out a constant volume calculation, rather than implementing more sophisticated procedures.[16]

As a first example we took a slab of four Co and four Zr planes; that is, 648 Co and 392 Zr atoms subject to periodic boundary conditions (PBC) in the x-y plane, but free in the z direction. For temperatures as low as $t = 0.10$ one already observes a strongly reduced $|S_{\mathrm{Co}}(\mathbf{K}, z)| < 0.2$ in the Co side of the interface, while the Zr planes remain practically unperturbed. Much the same holds true for $t = 0.12$, except that a qualitative change is observed in the Co pair-correlation function $g_2(r)$, which becomes smooth for the higher temperature value.

In contrast, a slab consisting of six Co and four Zr planes behaves quite differently. In fact the system remains periodic for temperatures up to $t = 0.20$, except for a slight degree of interface reconstruction. At $t = 0.24$ the structure factor $|S_{\mathrm{Co}}(\mathbf{K}, z)| \approx 0$, the Co interface pair-correlation function is quite smooth, and interface amorphization and interdiffusion are observed. However, bulk interdifusion remains negligible below this temperature.

Upon a further increase in system size to 12 Co and 10 Zr planes, that is, 1944 Co and 980 Zr atoms, it is observed that bulk periodicity is retained for temperatures up to $t = 0.27$. In fact, the histograms displayed in Fig. 1 show a sharp interface at $t = 0.21$, while at $t = 0.24$ some Co atoms have moved to the first Zr layer and vice versa. When $t = 0.27$ is reached some Co atoms have

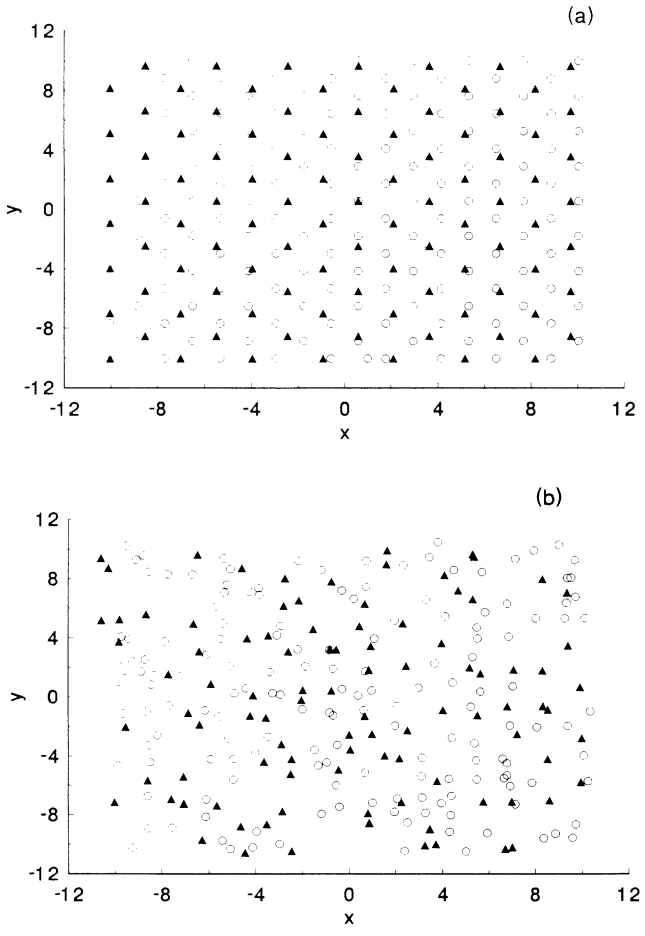

FIG. 2. Projection of the atomic positions on the x-y plane of the atoms within two lattice spacings of the original interface, at two different temperatures. As in Fig. 1 the Co and Zr atoms are denoted by open circles and full triangles, respectively. (a) $t = 0$ and (b) $t = 0.27$.

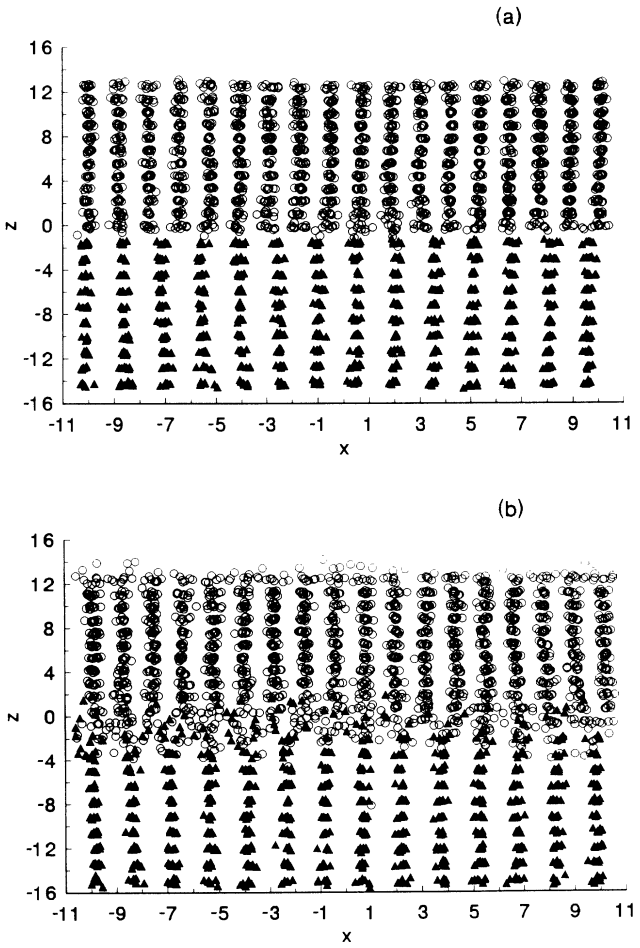

FIG. 3. Projection of the atomic positions on the x-z plane for two different temperatures. As in Fig. 1 the Co and Zr atoms are denoted by open circles and full triangles, respectively. (a) $t = 0.21$ and (b) $t = 0.27$.

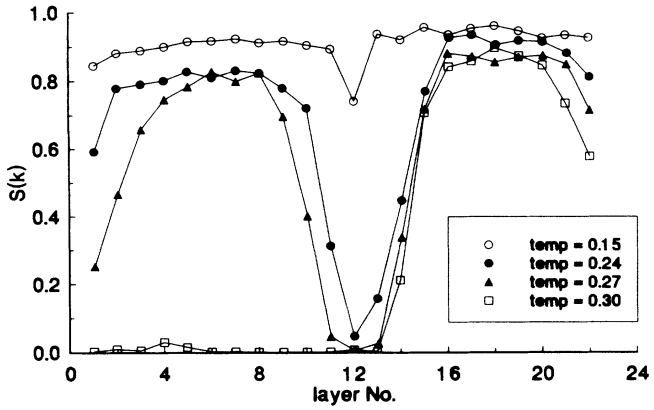

FIG. 4. Structure factor $S(\mathbf{K}, j)$ for several values of t vs the layer index j.

penetrated the second Zr layer, but bulk periodicity has not been significantly changed beyond this second layer. However, at $t = 0.30$ it is quite apparent that the Co side has lost periodicity and that atoms of both species have penetrated deeply into the other.

These features are further validated by Figs. 2 and 3, which depict the atomic positions after several thousand molecular-dynamics time steps. The disordering process, induced by increasing temperature, is clearly illustrated and easily visualized in these figures. Here and throughout, Co atoms are denoted by circles and Zr atoms by triangles. Figure 2 shows a projection of the atomic positions on the interface (x-y plane), of the atoms within two lattice spacings of the original interface. Figure 3 instead provides a projection of the atomic positions onto a (100), or x-z plane, perpendicular to the interface.

All the above peculiarities are corroborated by the structure factor $S(\mathbf{K}, z)$ of the Co layer next to the interface, which is portrayed in Fig. 4 for several values of the temperature t. It is observed that interface melting $[|S_{\mathrm{Co}}(\mathbf{K}, z_I)| = |S_{\mathrm{Zr}}(\mathbf{K}, z_I)| \approx 0$, where z_I stands for the interface layer] occurs at $t = 0.24$, while interdifusion starts at $t = 0.225$. Also the pair-correlation function $g_2(r)$, defined in Eq. (3.2) and displayed in Fig. 5 for $t = 0.15$ and 0.27, shows long-range order for the lower temperature, but only short-range order above $t = 0.27$. We have also contrasted these results with those obtained for a pure isolated Co slab, to check that the reduction of $|S_{\mathrm{Co}}(\mathbf{K}, z)|$, and the subsequent interface melting, actually develop for higher temperature than those reported above. In fact, for $t = 0.27$ the layers close to the surface exposed to vacuum remain ordered, while in Fig. 4 a significant reduction in the value of $|S_{\mathrm{Co}}(\mathbf{K}, z)|$, for z in the vicinity of the interface, is observed.

At this point it is quite clear to us that the system undergoes an order-disorder phase transition, with the gradual disappearance of long-range order, first at the interface and subsequently in the bulk. A more detailed understanding of the process is obtained through the scrutiny of Fig. 6, where we have plotted the mean square deviation of the atoms on the Co layer closest to the interface. At $t = 0.15$ a very small diffusion coefficient, conveying the concept of a solid, is obtained. On the other extreme, at $t = 0.30$ the calculation yields a value of $D \approx 6 \times 10^{-9}$ m^2/s, compatible with the liquid state.[12] However, at $t = 0.27$ the magnitude of the diffusion coefficient is 20 times smaller $D \approx 3 \times 10^{-10}$ m^2/s, and thus turns out to be consistent with the idea of an amorphous layer. Therefore, we understand that our results portray an order-disorder transition in which the fusion process nucleates around interface amorphization, and propagates from the interface towards the bulk, as the temperature increases.

Also the plot of total energy versus kinetic energy, displayed in Fig. 7, shows interesting features, which are compatible with the picture that emerged above. Up to $t = 0.24$ the slope is small and constant. A larger constant slope, consistent with interface amorphization, holds between $t = 0.24$ and 0.29. Above the latter a clearcut discontinuity, related to the solid–liquid transition, is observed.

The above characteristics, size-dependent melting temperature, interdiffusion, and interface amorphization, change only quantitatively when the calculations are performed under the imposition of periodic boundary conditions, as will be described in detail below.

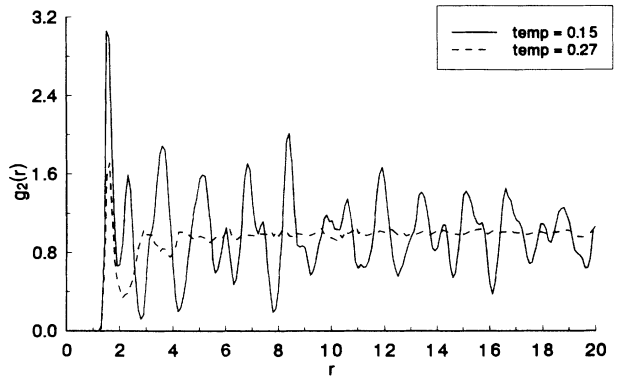

FIG. 5. Pair-correlation function $g_2(r)$ for $t = 0.15$ and 0.27.

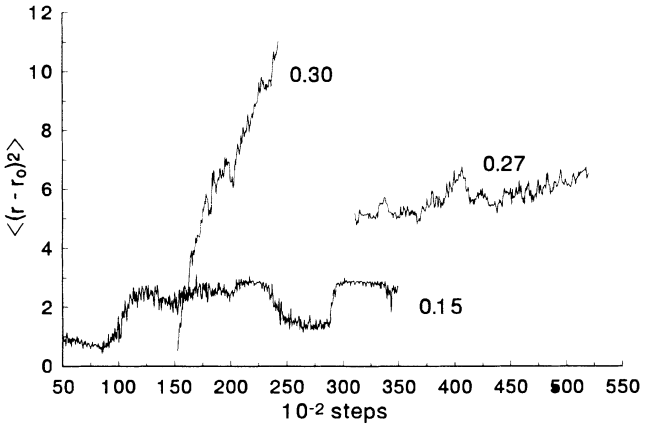

FIG. 6. Mean square deviation of the atoms on the Co layer closest to the interface for $t = 0.15$, 0.27, and 0.30.

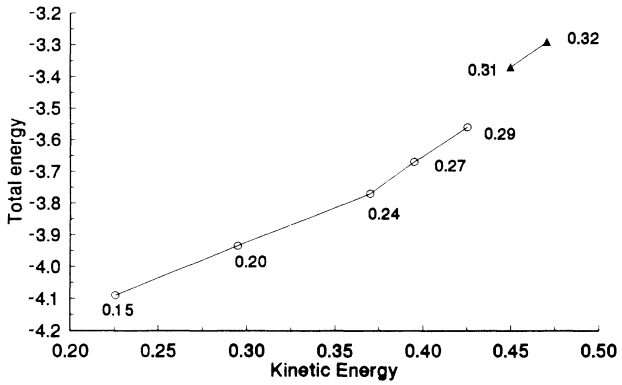

FIG. 7. Plot of total energy vs kinetic energy for various values of t.

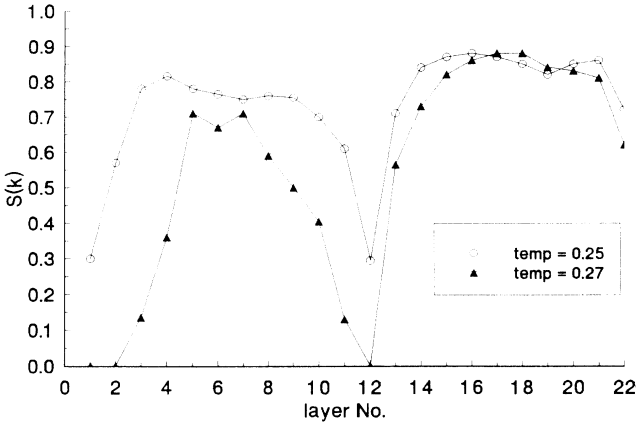

FIG. 9. Structure factor $S(\mathbf{K}, j)$, for $t = 0.25$ and 0.27 vs the layer index j for the periodic boundary conditions case.

B. Periodic boundary conditions

Again in this section we start reporting results of calculations made on small complexes and compare them with the corresponding ones obtained for larger systems. The smallest one we investigated consists of six Co and four Zr layers, subject to PBC in all three directions, and thus made up of 972 Co and 392 Zr atoms, 1364 particles in all. Under these conditions, and after 6000 time steps at a temperature of $t = 0.21$, the structure factor $S(\mathbf{K}, z)$ signals a complete melting of all the Co planes, while the Zr ones retain a certain degree of periodicity, as implied by $|S_{\mathrm{Zr}}(\mathbf{K}, z)| \approx 0.5$. The interfaces remain sharp, with no hint of interdiffusion. When the temperature is raised to $t = 0.25$ the preceding description remains valid, except for a *larger* value of $|S_{\mathrm{Zr}}(\mathbf{K}, z)|$, and the onset of interdifusion, both of Co into Zr and vice versa. For the two temperatures mentioned above, $t = 0.21$ and 0.25, the Co interface pair-correlation function $g_2(r)$ turns out to be quite smooth, implying interface amorphization.

When the size of the slab is increased to eight Co and six Zr planes, which corresponds to 1296 Co and 588 Zr atoms, the Co planes melt at the considerably higher temperature of $t = 0.25$, while the Zr ones retain a high degree of periodicity, except for the interface layer whose $|S_{\mathrm{Zr}}(\mathbf{K}, z)| \approx 0.5$. Interface atom interpenetration is observed, in the sense that a significant number of atoms of one species is found in what was originally the surface layer of the other, with even a few atoms of both elements interdiffusing into the bulk of the other. The Co interface pair-correlation function shows short-range order at $t = 0.21$, but becomes quite smooth at $t = 0.25$. The periodicity of the Zr surface and bulk structure is still present at $t = 0.32$.

When the system is further enlarged to 12 Co and 10 Zr planes, i.e., to 1944 Co and 980 Zr atoms, it still retains bulk periodicity at $t = 0.27$, as can be observed in the histogram of Fig. 8, which is quite similar to Fig. 1 for $t = 0.24$. On the other hand, interface disorder sets in close to $t = 0.27$, as can be deduced from inspection of Fig. 9, where the interface structure factor is displayed.

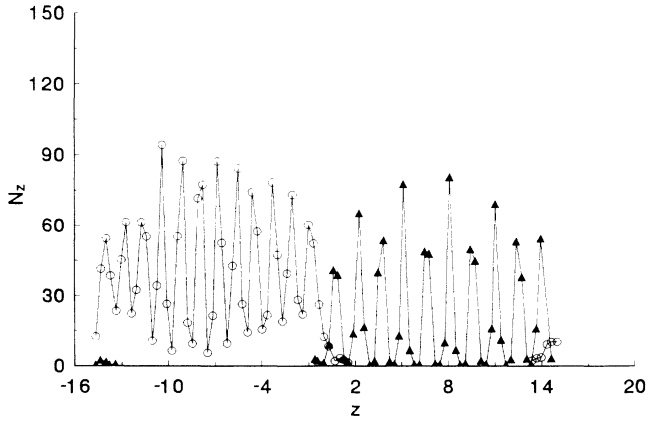

FIG. 8. Histograms of the spatial distribution of 1944 Co and 980 Zr atoms, denoted by open circles and full triangles, respectively, with periodic boundary conditions in the three spatial directions, and for $t = 0.27$.

IV. SUMMARY AND CONCLUSION

A Lennard-Jones molecular-dynamics simulation was implemented to model the atomic arrangement of an AB superlattice. We adopted for A and B the physical parameters of Co and Zr, respectively. However, while the crudeness of the Lennard-Jones potential does not allow us to model fully the metallic Co-Zr system, many trends obtained from our calculations are compatible with experiment. In fact, the Co-Zr superlattice becomes amorphous, according to the experimental results of Schröder, Samwer, and Koster,[6] due to a solid-state reaction, which is compatible with our results.

The overall picture which emerges from our calculations, and which applies to a class of systems dominated by atomic-size effects, can be summarized as follows. (i) As the temperature t increases interface amorphization develops, while the bulk remains periodic. (ii) Upon a further increase in temperature the disorder spreads

towards the bulk. (iii) At even higher values of t the whole system melts. (iv) These conclusions are robust, i.e., only quantitatively altered, by the adoption of either slab or periodic boundary conditions. (v) The characteristic of the process just described depend on the number of layers of the system adopted to carry out the molecular-dynamics computations. As expected, the temperatures for which the transitions occur scale with size, until the system becomes large enough to adequately model a macroscopic sample.

ACKNOWLEDGMENTS

This work was supported by the Fondo Nacional de Ciencia y Tecnología (FONDECYT), Chile, and the Departamento de Investigaciones de la Universidad Católica (DIUC). We gratefully acknowledge the assistance of the computing centers of ICTP (Trieste), where part of this work was completed, and that of PUC-Chile. Interesting discussions with Dr. Eduardo Savino are acknowledged.

[1]Proceedings of the Conference on Solid State Amorphizing Transformations, Los Alamos, New Mexico, 1987, edited by R. B. Schwartz, and W. L. Johnson, [J. Less-Common Met. **140** (1988)].
[2]R. B. Schwartz, and W. L. Johnson, Phys. Rev. Lett. **51**, 415 (1983).
[3]R. B. Schwartz, K. L. Wong, W. L. Johnson, and B. M. Clemens J. Non-Cryst. Solids **61&62**, 129 (1984).
[4]B. M. Clemens, W. L. Johnson, and R. B. Schwartz, J. Non-Cryst. Solids **61&62**, 817 (1984).
[5]See, for example, J. Phys. (Paris) Colloq. C4 (1990).
[6]H. Schröder, K. Samwer, and U. Koster, Phys. Rev. Lett. **54**, 197 (1985).
[7]S. Kobayashi and S. Takeuchi, J. Phys. F **14**, 23 (1984).
[8]A. Levi-Yeyati and M. Weissmann, Phys. Rev. B **35**, 2714 (1987).
[9]A. Levi-Yeyati M. Weissmann, and A. López-García, Phys. Rev. B **37**, 10608 (1988).
[10]F. H. Streitz, K. Sieradzki, and C. Cammarata, Phys. Rev. B **41**, 12285 (1990).
[11]S. J. Plimpton and E. D. Wolf, Phys. Rev. B **41**, 2712 (1990).
[12]C. Massobrio, V. Pontikis, and G. Martin, Phys. Rev. Lett. **62**, 1142 (1989).
[13]W. A. Harrison, *Electronic Structure, and the Properties of Solids* (Freeman, San Francisco, 1980).
[14]M. S. Daw and M. I. Baskes, Phys. Rev. B **29**, 6443 (1984).
[15]J. Rose, J. R. Smith, F. Guinea, and J. Ferrante, Phys. Rev. B **29**, 2963 (1984).
[16]J. F. Lutsko, D. Wolf, S. Yip, S. R. Philpot, and T. Nguyen, Phys. Rev. B **38**, 11572 (1988).
[17]S. R. Phillpot, S. Yip, and D. Wolf, Comput. Phys. **3** (6), 20 (1989).
[18]M. O. Robbins, G. S. Grest, and K. Kremer, Phys. Rev. B **42**, 5579 (1990).